

A Novel Arc Suppression Coil

Abstract. The arc suppression coil (ASC) is one of the most important devices in distribution networks to obtain the optimal power supply quality. Though there exists many types of ASC, some problems have been still not solved. In order to develop an ASC with rapid and continuous tuning and limited harmonics, this paper proposes a novel type of ASC, which is based on a single phase matrix converter. Due to pulse width modulation (PWM) control, compensating currents can be adjusted in a wide range and the order of harmonics is so high to be filtered easily. Finally, by using PSCAD/EMTDC, simulations are given to illustrate the feasibility and validity of this novel ASC.

Streszczenie. W artykule zaproponowano nowy typ dławika gaszącego ASC, bazujący na jednofazowym przekształtniku matrycowym. Dzięki modulacji PWM, możliwe jest generowanie prądów kompensujących o szerokim zakresie, a co za tym idzie skuteczna eliminacja harmonicznych. Wykonano badania symulacyjne w programie PSCAD/EMTDC, weryfikujące skuteczność działania rozwiązania. (**Dławik gaszący ASC**).

Keywords: Arc suppression coil, Resonant grounding, Compensated distribution network, Single-line-to-ground fault.

Słowa kluczowe: dławik gaszący, uziemienie rezonujące, sieć skompensowana, zwarcie doziemne jednofazowe.

Introduction

An arc suppression coils (ASC) is an adjustable reactor connected between the neutral point and the ground, which was invented by Petersen in 1916 to suppress the fault current between the fault point and the ground (consequently it is also called Petersen coil). When a single-line-to-ground (SLG) fault occurs, by properly tuning the ASC, a lagging reactive current from the ASC and a leading current from the line-to-ground capacitance can be made almost exactly equal, so that the fault current is substantially zero. Under this condition the arc can not maintain itself, and is made self-extinguishing [1-3].

It is beneficial that the circuit will remain connected without tripping circuit breakers in the event of a SLG fault. This solution offers many advantages such as significant and economical improvements in safety and power supply quality. Therefore, the ASC is widely used in the 6-35kV distribution networks in China.

Until now many kinds of ASCs have been applied in the MV distribution network. For example, plunger core coils require a precise mechanical drive system, have a long response time and many noise [3-5]. Winding turned ASCs respond more quickly and produce few harmonics, but can not continuously adjust the impedance [3, 6, 7]. Capacitor tuning ASCs use capacitors to cancel the inductive current generated from the reactor, but due to aging the capacitor value will become smaller as time goes on [8]. Magnetic controlled ASCs are more expensive [9-11]. Thyristor controlled ASCs overcome above drawbacks, but it is known that this kind of ASC generates low order harmonics. The unwanted low order harmonics are difficult to reduce [3, 12, 13].

In recent years some research scholars start to utilize the power electronic technology to design ASCs. [14] and [15] introduce an ASC based on transformer with controlled inverter load. The compensating current is generated by a DC/AC inverter. This voltage source pulse width modulation (PWM) inverter works as the secondary load of transformer, the reactance of the ASC can be regulated arbitrarily through controlling the inverter output current. However, one or more DC power is needed.

To overcome these drawbacks, this paper proposes a novel ASC, which is based on the single-phase matrix converter (SPMC) principle and the PWM technology.

The circuit topology and principles

As shown in Fig.1, the novel ASC consists of a single phase matrix converter (SPMC), a reactor, a 3-winding step-down transformer and a low-pass filter. If a neutral

point exists, the ASC can directly connect to it. If there is no wye point available for ASC connection to ground, an artificial neutral must be created on delta connection systems.

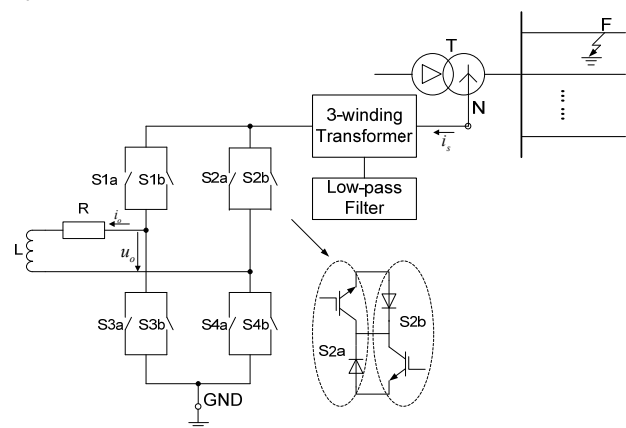


Fig.1. Simplified equivalent circuit diagram of a distribution network in the event of a SLG fault

The SPMC, which was first realized by Zuckerberger [16-18], is a forced commutated converter that uses an array of controlled bi-directional switches as the main power elements to create a variable output voltage system with unrestricted frequency. It does not have any dc-link circuit and does not need any large energy storage elements.

The SPMC consists of four bi-directional switches capable of blocking voltage and conducting current in both directions as show in Fig. 1 [16]. Because the bi-directional switch is not available to date, it can be implemented by connection of two diodes and two IGBTs in anti-parallel (common emitter back to back) as shown in Fig. 1. The IGBT were used because of its high switching capabilities and high current carrying capacities desirable for high-power applications.

Owing to limitations of low rated voltage of IGBT, a 3-winding step-down transformer is needed. The low-pass filter, which is connected to the tertiary winding, is used to filter high order harmonics in compensating currents. For the sake of clarity, the 3-winding transformer and the low-pass filter are negligible in the following discussion.

Gating signals are generated by comparing a reference signal u_r with a triangular carrier wave u_c of frequency f_c as shown in Fig. 2, where the symbols U_{cm} , U_{rm} are the peak amplitude of the carrier and the reference signal, respectively.

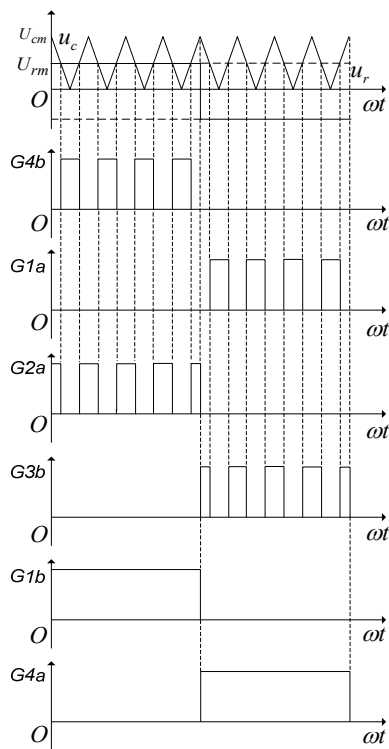


Fig.2. Gating signals of the bi-directional switches

If the output current i_o is greater than zero, the switch S_{1b} and S_{4b} turn on. The output current i_o passes through the neutral point N , the switch S_{1b} , R , L and another switch S_{4b} . The switch S_{4b} is controlled by PWM signals and in this positive half cycle, when S_{4b} is turned off, S_{2a} will be turned on and take the place of S_{4b} to provide a freewheeling path to discharge the stored energy.

If the output current i_o is lower than zero, the switch S_{1a} and S_{4a} turn on. The current i_o passes through the neutral point N , the switch S_{1a} , R , L and another switch S_{4a} . The switch S_{1a} is controlled by PWM signals and in this negative half cycle, when S_{1a} is turned off, the switch S_{3b} will be turn on and take the place of S_{4a} to provide a freewheeling path.

It's worth noting that gating signals of S_{2a} , S_{3b} are complement to that of S_{4b} , S_{1a} , respectively. In Fig. 2, G_{ia} and G_{ib} ($i=1, 2, 3, 4$) are the gating signals of S_{ia} and S_{ib} ($i=1, 2, 3, 4$), respectively.

Analysis of the working current

When a SLG fault occurs, the neutral voltage will increase, the size of which depends on the fault resistance. For simplicity, let the neutral voltage be

$$(1) \quad u_N = U_m \sin \omega t$$

where: U_m is the peak neutral voltage, $\omega=2\pi f$ and f is the frequency of the network. In the following analyses, switch devices as well as the diodes are considered as ideal elements. In Fig. 2, the triangular carrier u_c can be expressed as shown in (2).

$$(2) \quad u_c = \begin{cases} -\left[\omega t - (2k-1)\pi\right] \frac{U_{cm}}{\pi}, & \omega t \in [2(k-1)\pi, (2k-1)\pi) \\ \left[\omega t - (2k-1)\pi\right] \frac{U_{cm}}{\pi}, & \omega t \in [(2k-1)\pi, 2k\pi) \end{cases}$$

where: $\omega_c = 2\pi f_c$, $k=1, 2, 3, \dots$

Fig. 3 shows the k triangular carrier u_c crosses the reference signal u_r at points of α_k and β_k , which can be represented as shown in (3).

$$(3) \quad \begin{cases} \alpha_k = (2k-1)\pi - M\pi \\ \beta_k = (2k-1)\pi + M\pi \end{cases}$$

where: $k=1, 2, 3, \dots$ and M is define as the modulation factor, $M = U_{rm}/U_{cm}$. Obviously, $0 \leq M \leq 1$.

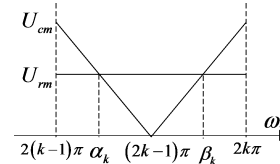


Fig.3. The triangular carrier u_c and the reference signal u_r

If $\alpha_k \leq \omega t \leq \beta_k$ ($k=1, 2, \dots, N/2$), the circuit is at ON state. The working current i_s flows into the ground through R and L . According to Kirchhoff's Voltage Law, the output current i_o can be solved from (4).

$$(4) \quad u_N = i_o R + L \frac{di_o}{dt}$$

With the initial condition described in (5), the solution of (4) is given as (6).

$$(5) \quad i_o(\omega t) \Big|_{\omega t = \alpha_k} = I_o(\alpha_k)$$

$$(6) \quad i_o = \frac{U_m}{|Z|} \sin(\omega t - \phi) + e^{-\frac{R}{\omega L}(\omega t - \alpha_k)} \left[I_o(\alpha_k) - \frac{U_m}{|Z|} \sin(\alpha_k - \phi) \right]$$

where the reactor impedance $Z=R+j\omega L$ and the angle $\phi = \arctan(\omega L/R)$.

At the end of the ON state in the steady state condition, $i_o(\beta_k) = I_o(\beta_k)$. With this condition applied to (6), the output current $I_o(\beta_k)$ is

$$(7) \quad I_o(\beta_k) = \frac{U_m}{|Z|} \sin(\beta_k - \phi) + e^{-\frac{R}{\omega L}(\beta_k - \alpha_k)} \times \left[I_o(\alpha_k) - \frac{U_m}{|Z|} \sin(\alpha_k - \phi) \right]$$

During the ON state, the working current i_s equals i_o as shown in (8).

$$(8) \quad i_s = i_o$$

If $2(k-1)\pi \leq \omega t \leq \alpha_k$ or $\beta_k \leq \omega t \leq 2k\pi$ ($k=1, 2, \dots, N/2$), the circuit is at OFF state. Similarly, with Kirchhoff's Voltage Law applied, the output current i_o can be solved from (9).

$$(9) \quad 0 = i_o R + L \frac{di_o}{dt}$$

The initial value of i_o at $\omega t = \beta_k$ is given in (7). Then the solution of (9) is got as (10).

$$(10) \quad i_o = I_o(\beta_k) e^{-\frac{R}{\omega L}(\omega t - \beta_k)}$$

At the end of the OFF state, $\omega t = \alpha_{k+1}$. The output current i_o is given as (11).

$$(11) \quad \begin{aligned} I_o(\alpha_{k+1}) &\triangleq i_o(\omega t) \Big|_{\omega t = \alpha_{k+1}} \\ &= I_o(\beta_k) e^{-\frac{R}{\omega L}(\alpha_{k+1} - \beta_k)} \end{aligned}$$

And this value is the initial value of the next ON state. During the OFF state, the working current i_s is zero as shown in (12).

$$(12) \quad i_s = 0$$

The two modes as described above are regularly repeated and the output current i_o is continuous, but the working current i_s is discontinuous. The waveforms of the output current i_o and the working current i_s during a switching period $[2(k-1)\pi, 2k\pi]$ are respectively given from (13) and (14).

$$(13) \quad i_o = \begin{cases} \frac{U_m}{|Z|} \sin(\omega t - \phi) + e^{-\frac{R}{\omega L}(\omega t - \alpha_k)} [I_o(\alpha_k) - \frac{U_m}{|Z|} \sin(\alpha_k - \phi)], & \alpha_k \leq \omega t \leq \beta_k \\ I_o(\beta_k) e^{-\frac{R}{\omega L}(\omega t - \beta_k)}, & \text{others} \end{cases}$$

$$(14) \quad i_s = \begin{cases} \frac{U_m}{|Z|} \sin(\omega t - \phi) + e^{-\frac{R}{\omega L}(\omega t - \alpha_k)} [I_o(\alpha_k) - \frac{U_m}{|Z|} \sin(\alpha_k - \phi)], & \alpha_k \leq \omega t \leq \beta_k \\ 0, & \text{others} \end{cases}$$

Harmonics analyses of the working current

Let an input $f_{in}(t) = F_m \sin \omega t$ be controlled by the PWM signals as shown in Fig. 2, the output $f_o(t)$ can be expressed as (15).

$$(15) \quad f_o(t) = \begin{cases} f_{in}(t), & \alpha_k \leq \omega t \leq \beta_k \\ 0, & \text{others} \end{cases}$$

According to the double Fourier series [19], the output $f_o(t)$ can be described in a Fourier series as shown in (16) or (17).

$$(16) \quad f_o(\omega t) = MF_m \sin \omega t + \sum_{n=1}^{\infty} (-1)^n \frac{F_m \sin nM\pi}{n\pi} \sin(\omega t \pm n\omega_c t)$$

$$(17) \quad f_o(\omega t) = F_m \sin \omega t \cdot g(\omega_c t)$$

where:

$$(18) \quad g(\omega_c t) = M + \sum_{n=1}^{\infty} (-1)^n \frac{2 \sin nM\pi}{n\pi} \cos n\omega_c t.$$

Thus, the output voltage u_o can be put in form of (19).

$$(19) \quad u_o = MU_m \sin \omega t + \sum_{n=1}^{\infty} (-1)^n \frac{U_m \sin nM\pi}{n\pi} \sin(\omega t \pm n\omega_c t)$$

Obviously, the fundamental component of the output voltage u_{o1} is

$$(20) \quad u_{o1} = MU_m \sin \omega t$$

The output current i_o can be yielded as (21).

$$(21) \quad i_o = \frac{MU_m \sin(\omega t - \chi_1)}{|Z_1|} + \frac{\sum_{n=1}^{\infty} (-1)^n \frac{U_m \sin nM\pi}{n\pi} \sin(\omega t \pm n\omega_c t - \chi_n)}{|Z_n|}$$

where: $Z_n = R + j\omega L$ and $\chi_n = \arctan(n\omega L/R)$ are the n harmonic impedance and its phase angle. For a special example, if $n=1$, $\chi_1 = \arctan(\omega L/R) = \phi$.

Similarly, the working current i_s can be derived from $i_s = i_o g(\omega_c t)$, then

$$(22) \quad i_s = \left[M + \sum_{n=1}^{\infty} (-1)^n \frac{2 \sin nM\pi}{n\pi} \cos n\omega_c t \right] \times \left[\frac{MU_m \sin(\omega t - \chi_1)}{|Z_1|} + \frac{\sum_{n=1}^{\infty} (-1)^n \frac{U_m \sin nM\pi}{n\pi} \sin(\omega t \pm n\omega_c t - \chi_n)}{|Z_n|} \right]$$

Thus, the fundamental component i_{s1} is

$$(23) \quad i_{s1} = \frac{M^2 U_m \sin(\omega t - \chi_1)}{|Z_1|}$$

It is obviously seen from (21) and (22) that the fundamental component of the output current i_o is linearly proportional to the modulation factor M , but that of the working current i_s is not. The value of fundamental working current i_s can be controlled in a wide range by adjusting the modulation factor M , which can be simply obtained by comparing a triangular wave with a reference signal. However, the working current i_s is not continual. When it is zero, the neutral point will become floating. Additionally, the ASC can only compensate the fundamental component of the fault current. So we can utilize filters to reduce harmonics and obtain the continual fundamental component.

The dominant harmonics of the current are near the switching frequency and its multiples ($\omega \pm n\omega_c$). Compared with thyristor controlled ASCs, due to the high switching frequency, these high order harmonics contents are more easily filtered. Therefore, only a low-pass filter can reduce the harmonics in the working current and maintain the continuity of compensating currents. This is one of advantages.

Simulations

This section consists of two parts: one is to verify the relationship between the working current of the ASC and the modulation factor M of the SPMC; the other is to validate the compensated effect of the ASC in a distribution network. The well-known PSCAD/EMTDC program was used to analyze how this ASC work [23].

Part 1: a voltage source with 5.774kV takes the place of the neutral voltage (In fact, the neutral voltage is nearly 5.774kV when a SLG fault occurs in a 10kV distribution network). Parameters in this simulation are listed in Table 1. By changing the modulation factor M , we can get different working currents as shown in Table 2, where the second column lists the fundamental component of working currents without the low-pass filter, while results shown in

the third column describes the effect of the low-pass filter. Obviously, due to the low-pass filter, the working current becomes smaller.

Table 1. The simulation parameters in Part 1

Reactor	$L=7.352$ mH
Step-down transformer	6/1.2/0.5 kV
Low-pass filter	$C_f=144$ μ F, $L_f=0.085$ mH

Table 2. Working currents

Modulation factor	No low-pass filter [A]	Low-pass filter [A]
0.1	1.1	0.6
0.2	4.0	2.6
0.3	9.0	7.1
0.4	16.1	13.4
0.5	25.1	20.9
0.6	36.2	29.4
0.7	49.2	38.6
0.8	64.1	48.1
0.9	81.0	57.8

Fig. 4 shows a 2-cycle wave of the working current in case of no low-pass filter and the modulation factor $M=0.7$. It is evident that the working current is not continuous and contains many harmonics. As result of a low-pass filter, the working current becomes smooth (Fig. 5).

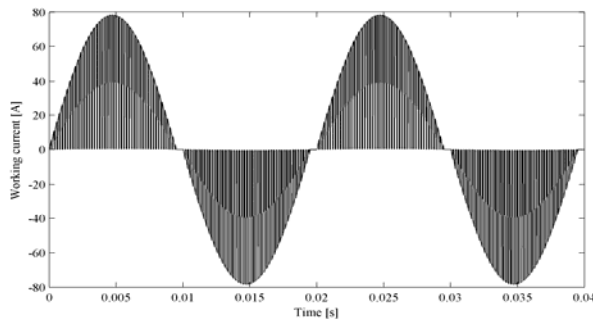


Fig.4 The working current (no low-pass filter)

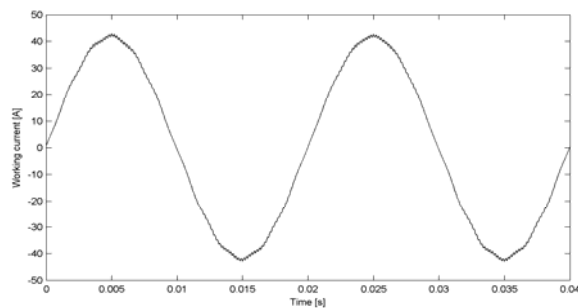


Fig. 5 The working current (with a low-pass filter)

Part 2: according to Fig. 1, a simple radial distribution network is constructed. This distribution network consists of 4 feeders. The power supply voltage is 10kV neglected the source impedance, which simulates an infinite power system. The length of each feeder is 2km, 6km, 12km and 13km respectively, whose parameters are as follows [24]: the positive sequence resistance $R_1=0.075\Omega/\text{km}$, the positive sequence inductance $L_1=0.254\text{mH}/\text{km}$ and the positive sequence capacitance $C_1=0.318\mu\text{F}/\text{km}$; the zero sequence resistance $R_0=0.102\Omega/\text{km}$, the zero sequence inductance $L_0=0.892\text{mH}/\text{km}$ and the zero sequence capacitance $C_0=0.210\mu\text{F}/\text{km}$.

A typical SLG fault was examined at the middle of the 13-km-long feeder. This simulation network has a total length of 33km, with the total capacitance current of 37.8A. According to Table 2, we should set the modulation factor $M=0.7$ so as to make the ASC work at a full-compensation state.

Fig. 6 and Fig. 7 show simulation results. When the SLG fault occurred at 0.103s, a transient over-current happened as shown in Fig. 6. Because of compensation of this novel ASC, the current-to-ground at the fault location drops from the maximum peak (165.1A) to 5.736A, to 3.239A, which are a small residual value (RMS<5A) as shown in Fig. 6. Therefore, the fault current can be limited to lower than 5A, so that the arc can not reignite. Due the fault resistance equals nearly zero, the neutral voltage increased to the phase voltage as shown in Fig. 7. When the fault disappeared at 0.410s, the neutral voltage decreases relatively slowly and it was not 866V (15% of the phase voltage 5.774kV) until $t=1.145\text{s}$ (Fig. 7). That is to say, the recovery voltage in the fault phase is likewise slow. This characteristic is very beneficial for the suppression of the arc reignition.

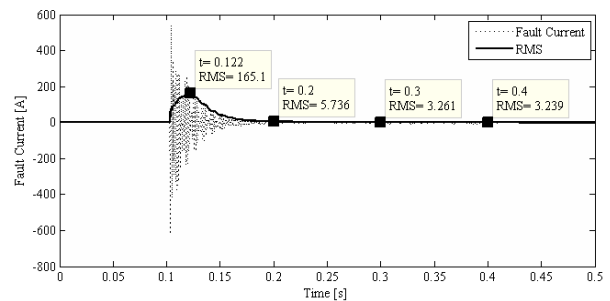


Fig. 6 The fault current and its own RMS (the fault occurred at 0.103s and lasted 0.307s)

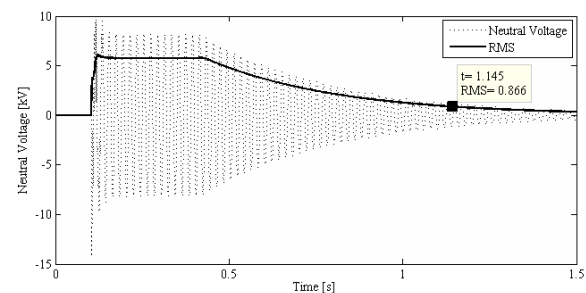


Fig. 7 The neutral voltage and its own RMS (the fault occurred at 0.103s and lasted 0.307s)

Conclusions

This paper presents a novel ASC, which is based on SPMC and PWM technology. Compared with other ASC such as winding turned ASC and the thyristor controlled ASC, this ASC not only can be continually tuned, but also generates much high order harmonic contents, which are easy to filter. If the value of the ASC is correctly tuned the current of a possible earth fault can be reduced to a suitable range. Simulations illustrate feasibility and validity.

The first author gratefully acknowledges the contributions of Baochang Xie, especially his valuable discussion on the original version of this document. This work was also supported in part by the Shanghai Science and Technology Development Foundation (No. 10dz1203902).

REFERENCES

- [1] ABB Electric Systems Technology Institute. *Electrical Transmission and Distribution Reference Book*. 5th ed. (1997)
- [2] Yao H. N., Cao M. Y., *Resonance to Ground in Power System*, China Electric Power Press, Beijing, China, (2000)
- [3] Product Department of State Grid Corporation of China, *A Booklet for implementing 10-66kV Arc Suppression Coil Management System*, China Electric Power Press, Beijing, China, (2006)
- [4] Brenna M., De Berardinis E., Delli Carpini L., etc., Petersen Coil Regulators Analysis Using a Real-Time Digital Simulator. *IEEE Transactions on Power Delivery*, 26 (2011), No. 3, 1479-1488
- [5] Pang Q. L., Sun T. J., Mu J., etc. Design of Air Gap Inductance Regulation Arc Suppression Coil Control System, *High Voltage Engineering*, 32 (2006), No. 4, 8-10
- [6] Leikermoser A., Ortolani F., New Techniques for Compensated Networks: Tuning the Petersen coil, Determining the Network Parameters and Performing Earth Fault Current Prediction and Reconstruction. *CIGRE 19th International Conference on Electricity Distribution*, paper 0120, 21-24 May, 2007, Vienna
- [7] Chen Z. R., Wu W. N., Zhang Q., Chen J. H., New Automatic Tuning Method for Multi-Tap Arc-Suppression Coil, *Automation of Electric Power Systems*, vol. 29 (2005), No. 12, 75-78
- [8] Xu Y. Q., Wang Z. Q., Zhang H., The Automatic Following Control of Arc Suppression Coil with Thyristor Switched Capacitors. *1st IEEE Conference on Industrial Electronics and Applications*, 24-26 May, 2006, Singapore
- [9] Cai X., Liu Y., Magnetic Bias Based Arc-Suppression Transformer with Three Phases and Five Columns and Its Tuning, *Automation of Electric Power Systems*, 28 (2004), No. 2, 83-88
- [10] Cai X., Liu Y., Hu C. Q., etc, New resonance earth system with magnetic bias and its protection, *Proceeding of the CSEE*, 24 (2004), No. 6, 44-49
- [11] Wu X., Cai X., Design of Key Parameters about Two-Stage Magnetic Valve Arc-Suppression Coil, *Diangong Jishu Xuebao*, 26 (2011), No. 10, 224-230
- [12] Chen H., Cai X., Wang J., Compensation Characteristics of Arc Suppressing Coil Controlled by TCR, *Automation of Electric Power Systems*, 31 (2007), No. 11, 81-86
- [13] Sun Y. Y., Zheng W. J., Xu W., A New Method to Model the Harmonic Generation Characteristics of the Thyristor Controlled Reactors. *IEEE Power Tech*, 1785-1790, 1-5 July, 2007, Lausanne
- [14] Zhang Y., Chen Q. F., Tian J., etc., Controllable Reactor Based on Transformer Winding Current Regulating, *Proceeding of the CSEE*, 29 (2009), No. 18, 113-118
- [15] Cheng L., Chen Q. F., Zhang Y., etc., Novel Arc-Suppression Coil Based on the Theory of Transformer with Controllable Load, *Automation of Electric Power Systems*, 30 (2006), No. 21, 77-81
- [16] Zuckerberger A., Weinstock D., Alexandrovitz A., Single-phase Matrix Converter, *IEE Proceedings Electric Power Applications*, 144 (1997), No. 4, 235-240
- [17] Agarwal V., Gupta S., An Efficient Algorithm for Generalised Single-phase Converter, *IET Power Electronics*, 3 (2010), No. 1, 138-145
- [18] Gola A. K., Agarwal V., Implementation of An Efficient Algorithm for A Single Phase Matrix Converter, *Journal of Power Electronics*, 9 (2009), No. 2, 198-206
- [19] Holmes D. G., Lipo T. A., *Pulse Width Modulation for Power Converter: Principles and Practice*, IEEE press, New York, USA, (2003)
- [20] Druml G., Kugi A., Seifert O., New Method to Control Petersen Coils by Injection of Two Frequencies, *CIGRE 18th International Conference and Exhibition on Electricity Distribution*, 1-5, 6-9 June, 2005, Turin, Italy
- [21] De Rybel T., Singh A., Pak P., Marti J. R., Online Signal Injection Through a Bus-Referenced Current Transformer, *IEEE Transactions on Power Delivery*, 25 (2010), No. 1, 27-34
- [22] Ortolani F., Leikermoser A., Neutral compensation and network monitoring - Test field experience in determining resonant point and homopolar parameters with active and passive pulse injection. *CIGRE 20th International Conference and Exhibition on Electricity Distribution*, 1-4, 8-11 June, 2009, Prague, Czech republic
- [23] Manitoba HVDC Research Centre Inc., PSCAD/EMTDC V4.2, www.pscad.com
- [24] Sun Y. M., Miao Y. Z., A New Principle of Transient Current Grounded Relay for Feeder in Resonant-Grounded Distribution Systems, *Proceeding of the CSEE*, 24 (2004), No. 3, 62-66

Authors: Bo XU, B111 Mulan Building, Shanghai Jiao Tong University, 800 Dongchuan Road, Shanghai 200240, China, E-mail: xuboshanghai@yahoo.cn; Jun ZHANG, B111 Mulan Building, Shanghai Jiao Tong University, 800 Dongchuan Road, Shanghai 200240, China, E-mail: junzhang@sjtu.edu.cn; Xu CAI, B111 Mulan Building, Shanghai Jiao Tong University, 800 Dongchuan Road, Shanghai 200240, China, E-mail: xucai@sjtu.edu.cn.